JGR Space Physics

Key Points:
- Weak magnetic storms cause notable modulation of the ionosphere-plasmasphere H^+ ion fluxes and prominent effects in the topside ionosphere
- The modulation is caused by the topside O^+ ion density changes induced by F2-layer peak up/down lifting
- F2-layer peak vertical motion is related to the changes in the B_z component of interplanetary magnetic field

Correspondence to:
D. V. Kotov,
dmitrykotoff@gmail.com

Weak Magnetic Storms Can Modulate Ionosphere-Plasmasphere Interaction Significantly: Mechanisms and Manifestations at Mid-Latitudes

D.V. Kotov[1] , P.G. Richards[2] , V. Truhlík[3] , N. Maruyama[4,5] , M. Fedrizzi[4,5] , M.O. Shulha[1,6], O.V. Bogomaz[1] , J. Lichtenberger[7,8] , M. Hernández-Pajares[9] , L.F. Chernogor[1] , L.Ya. Emelyanov[1] , T.G. Zhivolup[1], Ya.M. Chepurnyy[1], and I.F. Domnin[1]

[1]Institute of Ionosphere, Kharkiv, Ukraine, [2]Department of Computer Science, University of Alabama in Huntsville, Hunstville, Alabama, USA, [3]Institute of Atmospheric Physics of the Czech Academy of Sciences, Prague, Czech Republic, [4]Cooperative Institute for Research in Environmental Sciences, University of Colorado, Boulder, Colorado, USA, [5]NOAA Space Weather Prediction Center, Boulder, Colorado, USA, [6]National Technical University "Kharkiv Polytechnic Institute", Department of Radio Electronics, Kharkiv, Ukraine, [7]Department of Geophysics and Space Sciences, Eötvös Loránd University, Budapest, Hungary, [8]Geodetic and Geophysical Institute, RCAES, Hungarian Academy of Sciences, Budapest, Hungary, [9]UPC-IonSAT, IEEC-UPC, Universitat Politècnica de Catalunya, Barcelona, Spain

Abstract A comprehensive study of the response of the ionosphere-plasmasphere system at mid-latitudes to weak ($Dst_{min} > -50$ nT) magnetic storms is presented. For the first time, it is shown that weak magnetic disturbances can lead to significant modulation of ionosphere-plasmasphere H^+ ion fluxes. It is found that this modulation is caused by the enhancements/reductions of the topside O^+ ion density, which is induced by F2-layer peak height rise and fall during the storms. The F2-layer motion is caused by thermospheric wind changes and by a penetration electric field. Both drivers are closely related to the changes in the B_z component of interplanetary magnetic field. The most prominent manifestation of the H^+ ion flux modulation is strong changes in H^+ ion fraction in the topside ionosphere. This study also indicates that the NRLMSISE-00 model provides the correct relative changes of neutral H density during weak magnetic storms and also that there is a compelling need to include geomagnetic activity indices, in addition to solar activity ($F_{10.7}$), as input parameters to empirical topside ionosphere models.

1. Introduction

Although weak geomagnetic storms ($Dst_{min} > -50$ nT) occur much more frequently than strong ones (Loewe & Prölss, 1997), there are few studies devoted to their effects on the near-Earth plasma environment because their effects have traditionally been considered minor. The few studies of weak storm related effects at mid-latitudes primarily investigate the behavior of the key parameters h_mF_2, N_mF_2, and TEC (Buresova et al., 2014; Chen et al., 2014; Fedrizzi et al., 2008; Field et al., 1998; Goncharenko et al., 2006; Hajkowicz, 1999). They typically consider the interaction of the ionosphere with the thermosphere as the main cause of the observed effects.

The interaction of the ionosphere with the plasmasphere is very important in determining the state and behavior of both regions at mid-latitudes (e.g., Fok et al., 2005; Singh et al., 2011). Consequently, numerous studies have examined the effects of strong storms on the depletion of the plasmasphere and its refilling by plasma from the ionosphere (e.g., Chi et al., 2000; Foster et al., 2014; Reinisch et al., 2004). Others have studied the effects on the ionospheric electron temperature resulting from enhanced heat flows from ring current heating in the plasmasphere (Fok et al., 2005; Prölss, 2006).

In contrast, there has not been much research on weak storm impacts on the ionosphere-plasmasphere interaction at mid-latitudes. The statistical study of Förster and Jakowski (2000) revealed that weak magnetic storms in winter can cause a detectable (~20%) decrease of the night-time total electron content (TEC) at mid-latitudes, which they attributed to plasmasphere depletion during storms. Satellite observations discussed by Kotova et al. (2008) and Verigin et al. (2011) showed that moderate storms can lead to partial depletion of the plasmasphere. Kotov et al. (2018) studied the effects of the very weak storm of 24 December 2017 at Kharkiv (L = 2.1). They found that a significant reduction of the topside H^+ ion

density, TEC, and N_mF_2 at European mid-latitudes on the following night was caused by a partial depletion of the plasmasphere. Presumably, the root cause of such effects is the same as for strong storms. Several case studies report the changes in plasma temperature and O^+ and/or H^+ ion densities/fractions in the topside ionosphere during minor storms caused by high-speed solar wind streams (HSS). Heelis and Sojka (2011) and Hajra et al. (2017) suggested ionosphere expansion caused by HSS related heating of the thermosphere and ionosphere to be the main driver of the observed variations. The authors did not consider the possible role of changes in the ionosphere-plasmasphere interaction. In analyzing ten equinoxes during the minima of solar cycles 23/24, Kotov et al. (2015) found notable increases of the night-time upper transition height H_T (O^+/H^+) that coincided with the occurrence of weak magnetic disturbances. They also noted a strong positive correlation between H_T and h_mF_2. Such a correlation may be the result of the general expansion of the ionosphere caused by storm-time heating. On the other hand, because the topside ionosphere is the transition region between the ionosphere and plasmasphere (Banks et al., 1976), the effect may be a consequence of the changes in the ionosphere-plasmasphere interaction. This issue was not examined in the work of Kotov et al. (2015).

This study considers two periods that cover both the magnetically quiet and disturbed conditions and demonstrates that even weak magnetic storms are able to modulate the ionosphere-plasmasphere interaction, which may lead to important effects at mid-latitudes in the absence of plasmasphere depletion or significant heating of the thermosphere or ionosphere. We provide this confirmation by simulations with the field line interhemispheric plasma (FLIP) physical model that are constrained by selected Kharkiv incoherent scatter (IS) radar (Ukraine) data.

2. Research Tools

2.1. The Kharkiv IS Radar and Ionosonde

The Kharkiv IS radar (49.6°N, 36.3°E, L ≈ 2.1, solar apparent time LT ≈ UT + 2.4) uses a large zenith-directed 100-m diameter parabolic antenna and operates at 158-MHz carrier frequency. In the topside mode, the radar is capable of observing light ion (H^+ and He^+) fractions in addition to ion/electron temperatures and electron density. The observational data presented in this study were obtained with 20-min temporal resolution and with ~100-km altitude resolution. Such altitude resolution is acceptable for investigating the topside ionosphere (Kotov et al., 2015, Appendix). Data were obtained starting from an altitude of 200 km. To calibrate the electron density height profiles, f_oF_2 data from ionosonde located at the same observatory are used. The detailed descriptions on the radar mode and data analysis techniques are provided in the works of Kotov et al. (2015) and Bogomaz et al. (2017).

2.2. Digisonde at Grahamstown

In this study, we used the diurnal variations of h_mF_2 deduced from a digisonde ionograms at Grahamstown (33°S, 26°E), which is the station closest to Kharkiv's conjugate point. The digisonde data are taken at Global ionospheric radio observatory (GIRO; Reinisch & Galkin, 2011) portal (http://spase.info/SMWG/Observatory/GIRO). Before the inversion (Huang & Reinisch, 1996), the ionogram traces were checked manually to provide maximal accuracy of the h_mF_2 estimation.

2.3. FLIP Model

The FLIP model is a one-dimensional physical model of the coupled ionosphere and plasmasphere (Richards, 2001; Richards et al., 2000, 2010). A number of previous simulations with the FLIP model and the Kharkiv IS radar data revealed excellent model agreement with variations of the key ionospheric parameters over Kharkiv for all seasons at low solar activity (Kotov et al., 2015, 2016, 2018). In this study, we used a distinctive feature of the model—its ability to follow the measured F2-layer peak height (or horizontal wind velocity) and topside electron temperature T_e.

2.4. CTIPe Model

The Coupled Thermosphere Ionosphere Plasmasphere Electrodynamics (CTIPe) model is a global, three-dimensional coupled thermosphere-ionosphere-plasmasphere physics-based model (Codrescu et al., 2012; Fuller-Rowell et al., 1996). Among others, CTIPe simulate the time-dependent global structure of the wind vector. In this study, we used meridional component of horizontal wind provided by CTIPe version 3.2 hosted at the Community Coordinated Modeling Center (Shim et al., 2018).

2.5. TBT-15 Model

The TBT-15 model is an updated empirical model of the topside ion composition implemented in International Reference Ionosphere model-2016 (Bilitza et al., 2017; Truhlik et al., 2015). TBT-15 is based on the Atmosphere Explorer C&E, Intercosmos-24, and C/NOFS satellite data. The model input is index of solar activity $F_{10.7}$, and it outputs H^+, O^+, He^+, and N^+ ion fractions. In this study, we explain possible reasons for underestimation of the H^+ fraction by TBT-15 at mid-latitudes under magnetically quiet conditions.

3. Results and Discussions

For this study, we present two periods (23–25 September 2016 and 28–30 October 2004) during which there were three or more days of very quiet magnetic conditions followed by a weak magnetic disturbance and for which there were IS radar observational data for at least 24 hr before and after the beginning of the disturbance. The main solar wind parameters and indices of magnetic activity are shown in Figure 1. The solar activity was stable during these two periods with daily $F_{10.7}$ ~ 85–86 and 127–134, respectively. Unlike the cases of HSS studied by Heelis and Sojka (2011) and Hajra et al. (2017), the solar wind velocity was not high during the selected observation periods but there were some enhancements of the solar wind density. The AE index and B_z component of interplanetary magnetic field (IMF) were well correlated during both events: a southward turning of B_z precedes each of the enhancements in AE, and the northward turning of B_z precedes the decay of AE.

Comparison of the variations in the parameters of F2-layer peak and the topside ionosphere for both events (see Figures 2 and 3) during the disturbed periods with ones during the preceding 24 hr magnetically quiet periods shows the following. The storms did not affect the topside plasma temperatures significantly: maximal deviations did not exceed ~10% for T_i and ~20% for T_e. Changes of h_mF_2 were less than 15% and in N_mF_2 less than 45%. It is notable that the night-time vertical TEC values were almost unchanged (within ~2–3% for September 2016 and ~10% for October 2004); there was an increase on the second night of October 2004 period, most likely because of the increased N_mF_2. This implies that there were no significant depletions of the plasmasphere during the storms. The same conclusion follows for September 2016 from the measurements of the parameter which is more sensitive to the fullness/emptiness of the plasmasphere than the TEC—the mean electron density inside the altitude region 790–1,430 km computed from global dual-frequency GPS measurements in the daily-basis tomographic runs of UPC-IonSAT (Hernández-Pajares et al., 2017; Hernández-Pajares & Sanz, 1999). The density (not shown in the figures) obtained for the latitude of 46°N and inside the longitudinal region of 30–42°E has very close values (differences do not exceed ~7%) for all the three evenings and midnights of the considered September 2016 period. In contrast to the small changes in TEC, there was a prominent increase of the topside O^+ ion density (Figure 2) by factors of ~2–3.5 and a decrease of the H^+ ion fraction (Figure 4) by factors of ~1.8–2.5 during the nights following the beginning of the storms.

To understand the causes of such notable changes, we made two simulations with the FLIP model constrained by key observations. Both simulations began 5 days before the period of interest to allow the plasmasphere to reach equilibrium. The model was constrained to follow the measured topside T_e (Figure 3) in both simulations (Richards et al., 2000). The actual $F_{10.7}$ and 3-hr Kp indices were used in the NRLMSISE-00 model of neutral composition.

In the first simulation, the model was constrained to follow the observed h_mF_2 variations (Figure 2) to avoid uncertainties from empirical wind models. This calculation produced equivalent horizontal winds (Figure 4) that were then used in the second simulation.

Because the conjugate ionosphere also influences the density and temperature of the plasmasphere, the same procedure was applied to the southern hemisphere. The FLIP model followed the diurnal variations of h_mF_2 from a digisonde observation at Grahamstown (33°S, 26°E) whose location is close enough to the true conjugate point (38°S, 49°E).

Figure 2 shows the good agreement between the observed and simulated N_mF_2 for 23–25 September 2016, which supports the reliability of the NRLMSISE-00 O and N_2 densities for this period. There is some

underestimation of N_mF_2 by the FLIP model in October 2004 (up to ~30% during the quiet day and up to ~50% during the disturbed day) that likely implies that the actual O/N_2 ratio is higher than that provided by NRLMSISE-00. Additional simulations (not shown) indicate that a ~50 K reduction of T_n in NRLMSISE-00 improves the FLIP N_mF_2 significantly. The required decrease of T_n leads to a comparable decrease of the model T_i, which is within the error of the T_i measurements shown in Figure 3. It is important that the simulation shows that the changes in the topside ion densities caused by the 50 K reduction of T_n are negligible (~5%). Thus, the results in the topside and our conclusions will not be affected by this degree of T_n uncertainty.

For both September 2016 and October 2004, the FLIP model reproduces the diurnal variations of the topside O^+ and H^+ densities, and H^+ ion fraction very well when the H density in NRLMSISE-00 model was doubled (Figure 2). A multiplier of 2 was previously found to be needed for the equinoxes under low solar activity of 2006–2010 (Kotov et al., 2015) and of September 2016 (Kotov et al., 2018). Here we see that the same multiplier is adequate for October 2004 even though the solar activity was medium rather than low. The important point is that the H^+ density is reproduced well during both the quiet and disturbed periods of September 2016 and October 2004. This implies that NRLMSISE-00 model provided the correct storm-time relative changes of H density despite the actual absolute values being a factor of 2 higher during these periods.

In search of the causes of the strong H^+ fraction variability, it is helpful to consider chemical equilibrium where the H^+ density would be proportional to $[O^+][H]/[O]$. Our calculations (the results are plotted in Figure 2) show that the H^+ density obtained in this way differs significantly from the observations and simulation with FLIP—both quantitatively and qualitatively. For example, the chemical equilibrium H^+ ion density at each UT midnight of the 23–25 September 2016 period is not only much less than the actual H^+ ion density, but its changes are relatively small from night to night (within ~20%) when the actual change of H^+ density by the last night is a factor of 1.7 decrease. The reason of such stability is that despite the significant decrease in the [H]/[O] ratio from the first to the last night (by a factor of 3.8), this decrease is counterbalanced by a factor of 3.6 increase in $[O^+]$. A similar pattern is seen for the October 2004 period.

It is reasonable to attribute the difference between the observed and chemical equilibrium H^+ ion density in the topside ionosphere to the downward H^+ flux from the plasmasphere at night, which is a well-known phenomenon under these equinox conditions. Figure 4 confirms that the FLIP model H^+ flux at 1,000 km is downward at night and supplying additional H^+ ions to the topside ionosphere and increasing the H^+ density (Figure 2). The opposite case is seen in the morning, just after sunrise H^+ flux changes its direction to upward and the large number of chemically produced H^+ ions are taken out of the topside ionosphere and transported to the plasmasphere.

Substantial changes (enhancements or reductions) of the simulated H^+ flux are seen during the evenings of 24–25 September 2016 and 29 October 2004 (Figure 4) in comparison with the flux at the corresponding times during the magnetically quiet periods. This implies that the H^+ flux was modulated by the storms. It is seen (Figure 4) that the sharp changes (increase or decrease) of the observed H^+ ion fraction are coincident with the flux changes, that is, short-time H^+ ion fraction variations are apparently the signature of the modulation of ionosphere-plasmasphere H^+ flux.

The question becomes: what storm-related mechanism causes such significant modulation of the flux? The only plasma parameter that changes as much as the H^+ fraction is the topside O^+ density. It is seen that O^+ density and H^+ fraction changes are opposite and coincident in time (Figures 2 and 4). It is reasonable to hypothesize that the enhancement/reduction of O^+ density in the topside ionosphere reduces/enhances downward H^+ ion flux because the increasing/decreasing of the plasma pressure at the base of the plasmaspheric reservoir.

Then the question is, why are the topside O^+ density changes so strong during such weak storms? Thermal expansion/contraction of the ionosphere does not seem to be the explanation because there are no significant changes of T_e from evening to evening and T_i changes are too small to lead to significant changes of plasma scale height and to related notable changes of O^+ density in the topside ionosphere. Figure 2
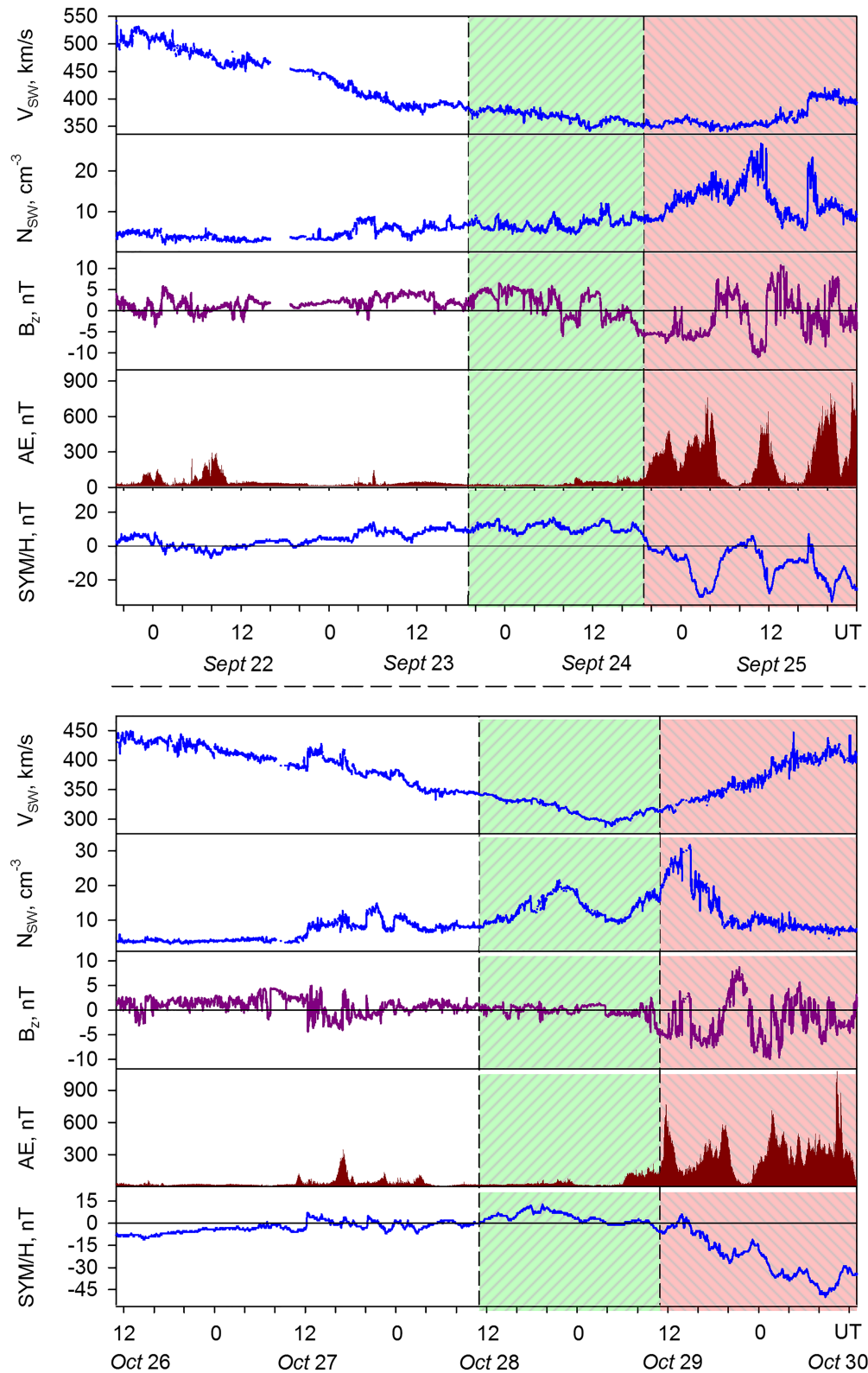
Figure 1. Variations of solar wind velocity (V_{SW}) and proton density (N_{SW}), the B_z component of interplanetary magnetic field, and the AE and SYM/H indices during 21–25 September 2016 (top panel) and 26–30 October 2004 (bottom panel). The Kharkiv IS radar measurement periods are indicated by the two shaded areas with two types of stripes. The first 24 hr of measurement (green shading with stripes '/') corresponds to magnetically quiet conditions. The rest of measurement (pink shading with stripes '\') corresponds to weakly disturbed conditions.
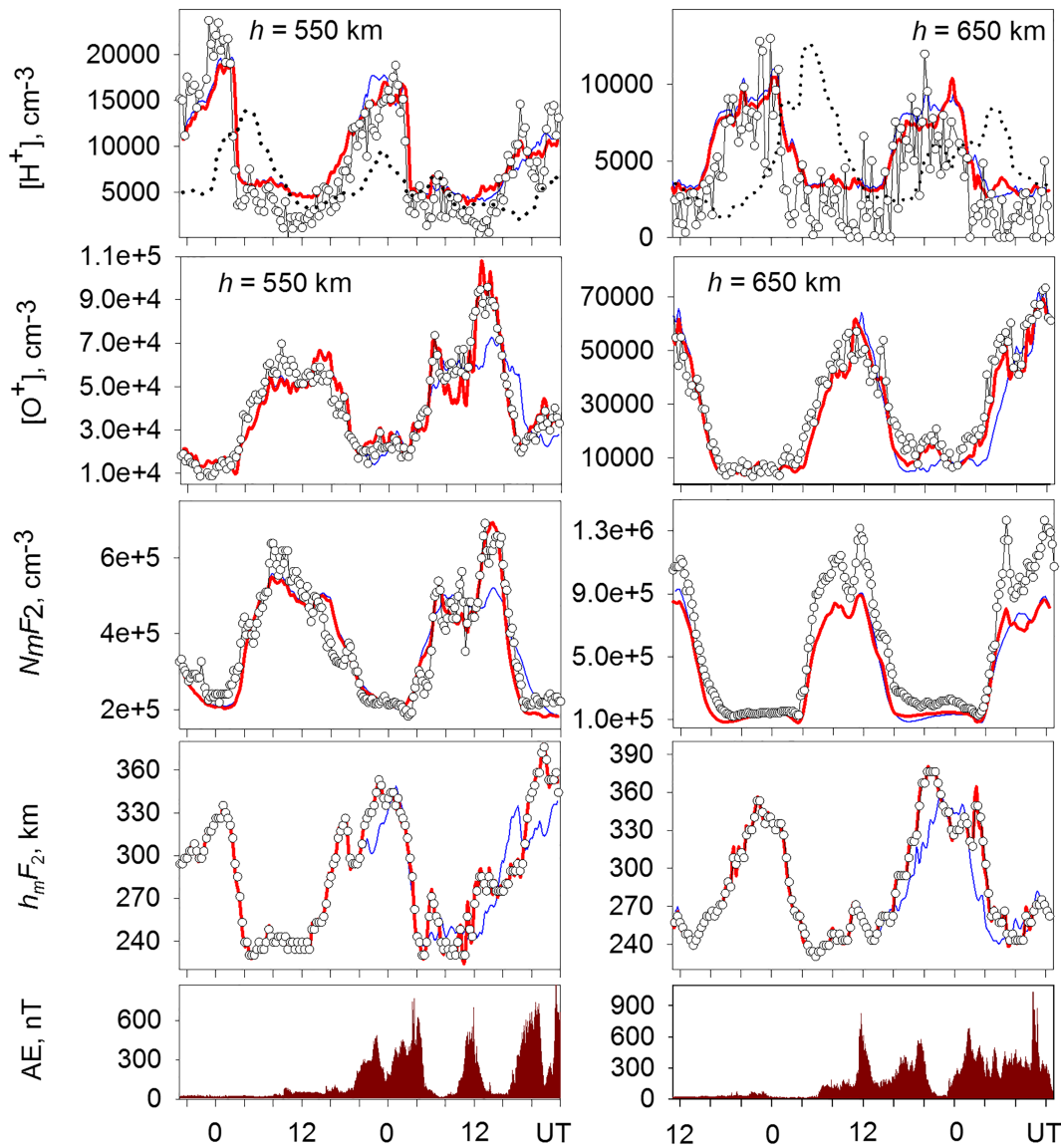
Figure 2. Observed (open circles) and FLIP model (lines) variations of F2-layer peak height (h_mF_2), peak electron density (N_mF_2), and the topside O^+ and H^+ ion densities during the quiet (first 24 hr) and enhanced (rest of the time) magnetic activity for 23–25 September 2016 (left panels) and 28–30 October 2004 (right panels). The thick red line denotes the FLIP simulation when the IS h_mF_2 is used as input in the northern hemisphere and the digisonde h_mF_2 is used as input in the southern hemisphere. The thin blue line shows the FLIP simulation when the quiet first day equivalent winds deduced from the measured h_mF_2 in both hemispheres are used as input for all days. Black dots show the calculations of the chemical equilibrium H^+ ion density.

shows that the O^+ density increases and decreases accompany the rise and fall of h_mF_2. Both rise and fall may be caused by changes of plasma transport due to changes in thermospheric winds or electric fields. Rises may also be caused by increases in neutral density by storm-induced heating of the thermosphere. To understand the contributions of changes of neutral density and plasma transport, we conducted a second simulation with the FLIP model.

In the second simulation, the FLIP model used the local time variations of the equivalent neutral winds in northern and southern hemispheres that were deduced from the measured h_mF_2 variations from the first 24 hr of observations, which had low magnetic activity. With the same quiet-time diurnal equivalent wind variation every day, any day-to-day changes in the topside ionosphere must be caused by storm effects on the neutral composition only. The results of this simulation are shown in Figures 2–4 by the thin blue line, and they clearly support the hypothesis on the role of O^+
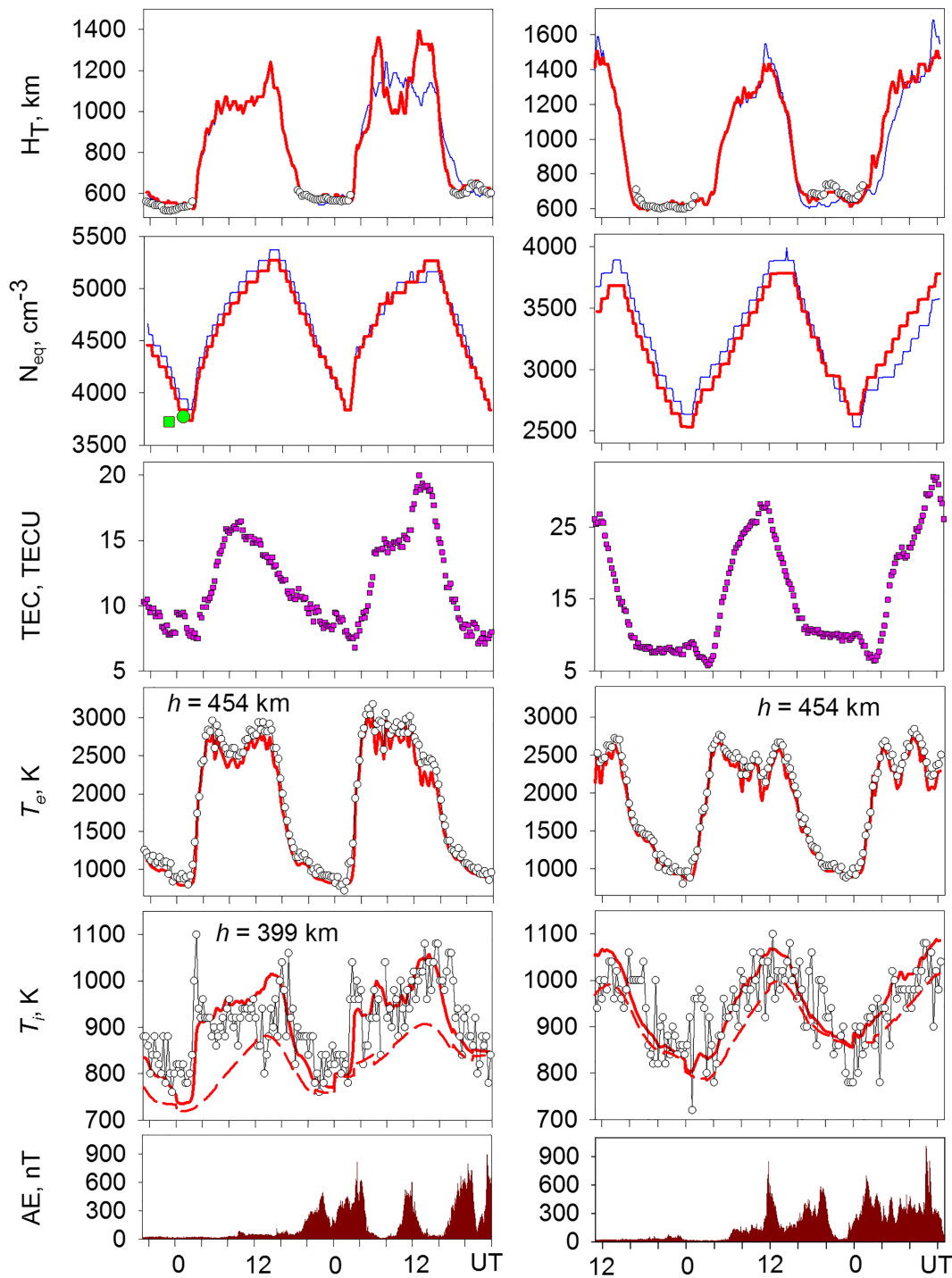
Figure 3. Diurnal variation of the topside T_i and T_e, plasmaspheric equatorial density N_{eq}, O^+/H^+ transition height, and TEC at 35°E provided by UPC global Ionospheric maps (Hernández-Pajares et al., 2017) for 23–25 September 2016 (left panels) and 28–30 October 2004 (right panels). Open circles show the observational results obtained with Kharkiv IS radar. The thick red line denotes the FLIP simulation when the IS h_mF_2 is used as input in the northern hemisphere and the digisonde h_mF_2 is used as input in the southern hemisphere. The thin blue line shows the FLIP simulation when the quiet first day equivalent winds deduced from the measured h_mF_2 in both hemispheres are used as input for all days. The dashed red line shows T_n from the NRLMSISE-00 model. Green symbols denote the N_{eq} values based on the values obtained from whistler observations with the AWDA system (Lichtenberger et al., 2010) at Tihany (46.9°N, 17.9°E) at 00:00:06 UT (circle) and at Grahamstown (33.3°S, 26.5°E) at 02:38:27 UT (square) of September 23, 2016. Because the N_{eq} at Tihany and Grahamstown were obtained for L = 2.4 flux tubes, they were corrected for the Kharkiv's flux tube (L = 2.1) using $N_{eq} \sim L^{-3.07}$ law (Ozhogin et al., 2012). The corrected N_{eq} is plotted with UT, which corresponds at Kharkiv to the same magnetic local times as for the whistler observatories.
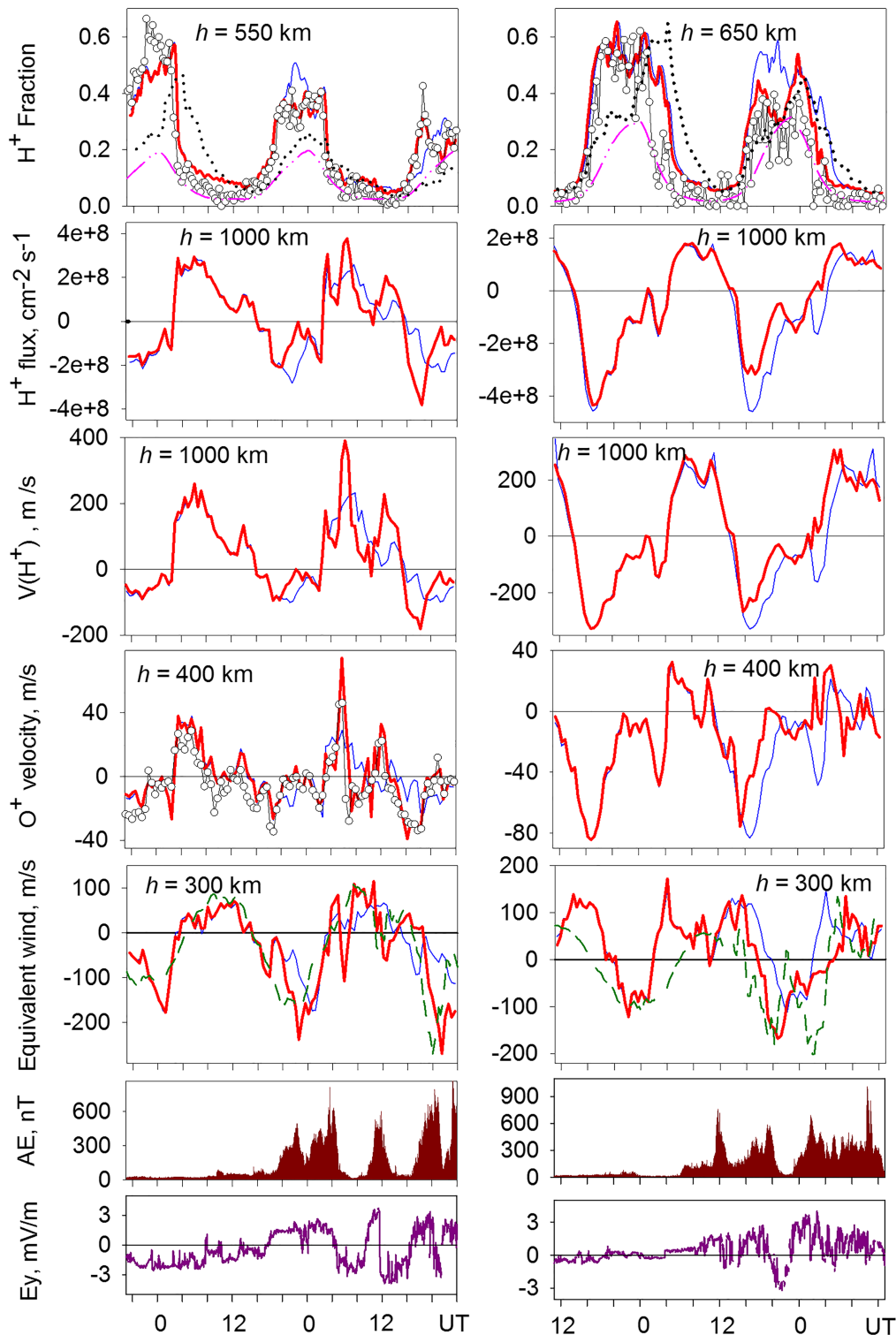
Figure 4. Diurnal variations of zonal component of magnetospheric electric field E_y, AE index, equivalent meridional horizontal wind velocity at 300 km, O^+ ion velocity at 400 km, and H^+ ion velocity and flux at 1,000 km for 23–25 September 2016 (left panels) and 28–30 October 2004 (right panels). Open circles show the observational results obtained with Kharkiv IS radar. The thick red line denotes the FLIP simulation when the IS h_mF_2 is used as input in the northern hemisphere and the digisonde h_mF_2 is used as input in the southern hemisphere. The thin blue line shows the FLIP simulation when the quiet first day equivalent winds deduced from the measured h_mF_2 in both hemispheres are used as input for all days. The dashed dark green line is the meridional horizontal wind velocity at 300 km from the CTIPe model. Black dots show the H^+ fraction calculated with the chemical equilibrium H^+ ion density. The dash-dotted pink lines show the H^+ fraction from the new TBT-15 empirical model of topside ion composition that is included in the International Reference Ionosphere model (IRI-2016).

density impact on ionosphere-plasmasphere H^+ ion flux. It is seen that the changes of h_mF_2 are almost fully caused by the plasma transport changes (seen in the equivalent wind velocity, Figure 4), and they really lead to remarkable changes in the H^+ flux. As a result, there are sharp changes of the observed H^+ ion fraction during the periods with weakly disturbed magnetic activity in both September 2016 and October 2004. It is interesting also to note the strong similar effects for the morning and daytime hours of 25 September 2016. These effects are not seen with the IS observations because of the low daytime H^+ fraction at the altitudes available for the measurements; however, the FLIP model shows ~250 km increase and ~200 km decrease of the O^+/H^+ ion upper transition height coincident with modulation of the upward H^+ ion flux that was induced by the motion of F2-layer and related changes of the topside O^+ ion density. It should be noted also that comparison of the observed and simulated variations of the vertical O^+ ion velocity in the topside ionosphere additionally supports this conclusion very well (Figure 4).

The final question is, how is the O^+ ion motion driven by weak magnetic disturbances? Comparison of the variations of equivalent wind, vertical O^+ ion velocity, AE index, and the zonal component of magnetospheric electric field E_y (Figure 4) suggests two possible causes of O^+ ion motion for both events we consider. First, an enhanced thermospheric wind is caused by enhanced auroral heating. Second, ExB drift caused by penetration of the magnetospheric electric field just after the times when the field changes its direction or value. We have made simulations of the horizontal thermospheric wind with the CTIPe model (Codrescu et al., 2012; Fuller-Rowell et al., 1996) to clarify the main driver. Variations of meridional component of the horizontal thermospheric wind from the CTIPe model (Figure 4) follow the general changes of equivalent wind deduced from the observations with the FLIP model very well starkly illustrating the dominant role of changes in the thermospheric wind on the O^+ ion vertical transport. The differences between the CTIPe winds and FLIP model equivalent winds that are seen just before UT midnight of 25 September and after 01:30 UT on 30 October may indicate the presence of a penetration magnetospheric electric field. The changes of the FLIP equivalent wind during these time intervals agree with the changes of the E_y component direction just before.

It should be emphasized that the simulated H^+ ion velocity changes are much higher than ones for the O^+ velocity (Figure 4). This means again that the H^+ flux modulation is really governed by the F2-layer motion because ExB drift of the plasma as a whole would lead to the same velocities for both H^+ and O^+ ions.

Given that thermospheric winds are strongly affected by auroral activity and that there is high correlation between the AE index and B_z component of IMF as noted above, variations in B_z can be considered the primary cause of the modulation of the plasmasphere-ionosphere H^+ flux. It is well known that E_y is also governed by the behavior of the IMF B_z.

Comparison of our H^+ ion fraction results with the calculations from the new empirical model of the topside ion composition TBT-15 (Bilitza et al., 2017) reveals an interesting feature. Namely, the model H^+ fraction is underestimated by a factor of 2–3 (Figure 2) during the quiet periods, but it fits the observations very well during the disturbances. This supports our previous hypothesis that the reason for the empirical model H_T being too high for solar minimum is that it is based on data collected during 1974 when there were frequent minor geomagnetic disturbances (Kotov et al., 2015). The present work shows that such disturbances do lead to significant reduction of the H^+ ion fraction.

4. Conclusions

This comprehensive study of two weak storm events has revealed the following:

1. Sharp prominent changes of the observed H^+ ion fraction in the topside ionosphere are a strong signature of the modulation of ionosphere-plasmasphere H^+ flux.
2. Even weak magnetic disturbances lead to significant modulation of ionosphere-plasmasphere H^+ ion fluxes. This modulation is caused by variations in the topside O^+ ion density caused by the h_mF_2 motion most likely induced by changes of the thermospheric horizontal wind, but also possibly by magnetospheric penetrated electric fields. Both mechanisms are closely related to the changes in the IMF B_z component.

3. The strong sensitivity of the topside H^+ ion fraction to very weak magnetic disturbances indicates the need to include geomagnetic activity indices as input parameters to empirical topside ionosphere composition models.

4. Comparison of the observed and simulated H^+ ion density variations in the topside ionosphere indicates that the NRLMSISE-00 model provides the correct relative changes of neutral H density during these storm events even though it underestimates the absolute density by a factor of 2 for both the considered periods.

References

Banks, P. M., Schunk, R. W., & Raitt, W. J. (1976). The topside ionosphere: A region of dynamic transition. *Annual Review of Earth and Planetary Sciences, Vol.*, *4*, 381–440. https://doi.org/10.1146/annurev.ea.04.050176.002121

Bilitza, D., Altadill, D., Truhlik, V., Shubin, V., Galkin, I., Reinisch, B., & Huang, X. (2017). International reference ionosphere 2016: From ionospheric climate to real-time weather predictions. *Space Weather*, *15*, 418–429. https://doi.org/10.1002/2016SW001593

Bogomaz, O., Kotov, D., Panasenko, S., & Emelyanov, L. (2017, September). Advances in software for analysis of Kharkiv incoherent scatter radar data. In *2017 International Conference on Information and Telecommunication Technologies and Radio Electronics (UkrMiCo)*, (pp. 1–5). IEEE. https://doi.org/10.1109/UkrMiCo.2017.8095425

Buresova, D., Lastovicka, J., Hejda, P., & Bochnicek, J. (2014). Ionospheric disturbances under low solar activity conditions. *Advances in Space Research*, *54*(2), 185–196. https://doi.org/10.1016/j.asr.2014.04.007

Chen, Y., Liu, L., Le, H., & Wan, W. (2014). Geomagnetic activity effect on the global ionosphere during the 2007–2009 deep solar minimum. *Journal of Geophysical Research: Space Physics*, *119*, 3747–3754. https://doi.org/10.1002/2013JA019692

Chi, P. J., Russell, C. T., Musman, S., Peterson, W. K., Le, G., Angelopoulos, V., et al. (2000). Plasmaspheric depletion and refilling associated with the September 25, 1998 magnetic storm observed by ground magnetometers at L = 2. *Geophysical research letters*, *27*(5), 633–636. https://doi.org/10.1029/1999GL010722

Codrescu, M. V., Negrea, C., Fedrizzi, M., Fuller-Rowell, T. J., Dobin, A., Jakowsky, N., et al. (2012). A real-time run of the Coupled Thermosphere Ionosphere Plasmasphere Electrodynamics (CTIPe) model. *Space Weather*, *10*, S02001. https://doi.org/10.1029/2011SW000736

Fedrizzi, M., Fuller-Rowell, T. J., Maruyama, N., Codrescu, M., & Khalsa, H. (2008). Sources of F-region height changes during geomagnetic storms at mid latitudes. *Washington DC American Geophysical Union Geophysical Monograph Series*, *181*, 247–258. https://doi.org/10.1029/181GM22

Field, P. R., Rishbeth, H., Moffett, R. J., Wenden, D. W., Fuller-Rowell, T. J., Millward, G. H., & Aylward, A. D. (1998). Modelling composition changes in F-layer storms. *Journal of Atmospheric and Solar-Terrestrial Physics*, *60*(5), 523–543. https://doi.org/10.1016/S1364-6826(97)00074-6

Fok, M. C., Ebihara, Y., & Moore, T. E. (2005). Inner magnetospheric plasma interactions and coupling with the ionosphere. *Adv. Polar Upper Atmos. Res.*, *19*, 106–134.

Förster, M., & Jakowski, N. (2000). Geomagnetic storm effects on the topside ionosphere and plasmasphere: A compact tutorial and new results. *Surveys in Geophysics*, *21*(1), 47–87. https://doi.org/10.1023/A:1006775125220

Foster, J. C., Erickson, P. J., Coster, A. J., Thaller, S., Tao, J., Wygant, J. R., & Bonnell, J. W. (2014). Storm time observations of plasmasphere erosion flux in the magnetosphere and ionosphere. *Geophysical Research Letters*, *41*, 762–768. https://doi.org/10.1002/2013GL059124

Fuller-Rowell, T. J., Rees, D., Quegan, S., Moffett, R. J., Codrescu, M. V., & Millward, G. H. (1996). In R. W. Schunk (Ed.), *STEP Handbook on Ionospheric Models*. Utah State University.

Goncharenko, L., Salah, J., Crowley, G., Paxton, L. J., Zhang, Y., Coster, A., et al. (2006). Large variations in the thermosphere and ionosphere during minor geomagnetic disturbances in April 2002 and their association with IMF By. *Journal of Geophysical Research Space Physics*, *111* A03303(A3). https://doi.org/10.1029/2004JA010683

Hajkowicz, L. A. (1999). Monitoring ionospheric response to auroral electrojet activity from sub-auroral to equatorial latitudes in the East Asian-Australian longitudinal sector over a solar cycle (1978–1986). *Journal of atmospheric and solar-terrestrial physics*, *61*(11), 857–866. https://doi.org/10.1016/S1364-6826(99)00034-6

Hajra, R., Tsurutani, B. T., Brum, C. G., & Echer, E. (2017). High-speed solar wind stream effects on the topside ionosphere over Arecibo: A case study during solar minimum. *Geophysical Research Letters*, *44*, 7607–7617. https://doi.org/10.1002/2017GL073805

Heelis, R. A., & Sojka, J. J. (2011). Response of the topside ionosphere to high-speed solar wind streams. *Journal of Geophysical Research Space Physics*, *116* A11314(A11). https://doi.org/10.1029/2011JA016739

Hernández-Pajares, M., Roma-Dollase, D., Krankowski, A., García-Rigo, A., & Orús-Pérez, R. (2017). Methodology and consistency of slant and vertical assessments for ionospheric electron content models. *Journal of Geodesy*, *91*(12), 1405–1414. https://doi.org/10.1007/s00190-017-1032-z

Hernández-Pajares, M., Juan, J. M., & Sanz, J. (1999). New approaches in global ionospheric determination using ground GPS data. *Journal of Atmospheric and Solar-Terrestrial Physics*, *61*, 1237–1247. https://doi.org/10.1146/annurev.ea.04.050176.002121

Huang, X., & Reinisch, B. W. (1996). Vertical electron density profiles from the digisonde network. *Advances in Space Research*, *18*(6), 121–129. https://doi.org/10.1016/0273-1177(95)00912-4

Kotov, D. V., Richards, P. G., Bogomaz, O. V., Chernogor, L. F., Truhlík, V., Emelyanov, L. Y., et al. (2016). The importance of neutral hydrogen for the maintenance of the midlatitude winter nighttime ionosphere: Evidence from IS observations at Kharkiv, Ukraine, and field line interhemispheric plasma model simulations. *Journal of Geophysical Research: Space Physics*, *121*, 7013–7025. https://doi.org/10.1002/2016JA022442

Kotov, D. V., Richards, P. G., Truhlík, V., Bogomaz, O. V., Shulha, M. O., Maruyama, N., et al. (2018). Coincident observations by the Kharkiv IS radar and ionosonde, DMSP and Arase (ERG) satellites, and FLIP model simulations: Implications for the NRLMSISE-00 hydrogen density, plasmasphere, and ionosphere. *Geophysical Research Letters*, *45*(16), 8062–8071. https://doi.org/10.1029/2018GL079206

Kotov, D. V., Truhlík, V., Richards, P. G., Stankov, S., Bogomaz, O. V., Chernogor, L. F., & Domnin, I. F. (2015). Night-time light ion transition height behaviour over the Kharkiv (50°N, 36°E) IS radar during the equinoxes of 2006–2010. *Journal of Atmospheric and Solar-Terrestrial Physics*, *132*, 1–12. https://doi.org/10.1016/j.jastp.2015.06.004

Kotova, G., Bezrukikh, V., Verigin, M., & Smilauer, J. (2008). New aspects in plasmaspheric ion temperature variations from INTERBALL 2 and MAGION 5 measurements. *Journal of Atmospheric and Solar-Terrestrial Physics*, *70*, 399–406. https://doi.org/10.1016/j.jastp.2007.08.054

Lichtenberger, J., Ferencz, C., Hamar, D., Steinbach, P., Rodger, C. J., Clilverd, M. A., & Collier, A. B. (2010). Automatic whistler detector and analyzer system: Implementation of the analyzer algorithm. *Journal of Geophysical Research Space Physics*, *115*(A12). https://doi.org/10.1029/2010JA015931

Loewe, C. A., & Prölss, G. W. (1997). Classification and mean behavior of magnetic storms. *Journal of Geophysical Research.*, *102*(A7), 14209–14213. http://doi.org/10.1029/96JA04020

Ozhogin, P., Tu, J., Song, P., & Reinisch, B. W. (2012). Field-aligned distribution of the plasmaspheric electron density: An empirical model derived from the IMAGE RPI measurements. *Journal of Geophysical Research.*, *117*, A06225. https://doi.org/10.1029/2011JA017330

Prölss, G. W. (2006, August). Subauroral electron temperature enhancement in the nighttime ionosphere. *Annales Geophysicae*, *24*(7), 1871–1885. https://doi.org/10.5194/angeo-24-1871-2006

Reinisch, B. W., & Galkin, I. A. (2011). Global ionospheric radio observatory (GIRO). *Earth, Planets, and Space*, *63*, 377–381. https://doi.org/10.5047/eps.2011.03.001

Reinisch, B. W., Huang, X., Song, P., Green, J. L., Fung, S. F., Vasyliunas, V. M., et al. (2004). Plasmaspheric mass loss and refilling as a result of a magnetic storm. *Journal of Geophysical Research Space Physics*, *109* A01202(A1). https://doi.org/10.1029/2003JA009948

Richards, P. G. (2001). Seasonal and solar cycle variations of the ionospheric peak electron density: Comparison of measurement and models. *Journal of Geophysical Research*, *106*(A7), 12,803–12,819. https://doi.org/10.1029/2000JA000365

Richards, P. G., Bilitza, D., & Voglozin, D. (2010). Ion density calculator (IDC): A new efficient model of ionospheric ion densities. *Radio Science*, *45*, RS5007. https://doi.org/10.1029/2009RS004332

Richards, P. G., Buonsanto, M. J., Reinisch, B. W., Holt, J., Fennelly, J. A., Scali, J. L., et al. (2000). On the relative importance of convection and temperature on the behavior of the ionosphere in North America during January, 6–12, 1997. *Journal of Geophysical Research Space Physics*, *105*, 12,763–12,776. https://doi.org/10.1029/1999ja000253

Shim, J. S., Tsagouri, I., Goncharenko, L., Rastaetter, L., Kuznetsova, M., Bilitza, D., et al. (2018). Validation of ionospheric specifications during geomagnetic storms: TEC and foF2 during the 2013 March storm event. *Space Weather*, *16*, 1686–1701. https://doi.org/10.1029/2018SW002034

Singh, A. K., Singh, R. P., & Siingh, D. (2011). State studies of Earth's plasmasphere: A review. *Planetary and Space Science*, *59*(9), 810–834. https://doi.org/10.1016/j.pss.2011.03.013

Truhlik, V., Bilitza, D., & Triskova, L. (2015). Towards better description of solar activity variation in the International Reference Ionosphere topside ion composition model. *Advances in Space Research*, *55*(8), 2099–2105. https://doi.org/10.1016/j.asr.2014.07.033

Verigin, M. I., Kotova, G. A., Bezrukikh, V. V., Bogdanov, V. V., & Kaisin, A. V. (2011). Ion drift in the Earth's inner plasmasphere during magnetospheric disturbances and proton temperature dynamics. *Geomagnetism and Aeronomy*, *51*(1), 39–48. https://doi.org/10.1134/s0016793211010154